C. van Lookeren Campagne
Research Engineer

R. Nicodemus
Research Engineer

Robert Bosch GmbH,
Postfach 300 240,
D-70442 Stuttgart, Germany

G. J. de Bruin[1]
Research Engineer

D. Lohse
Professor

The University of Twente,
Department Applied Physics,
PO Box 217,
NL 7500 AE Enschede, Netherlands

A Method for Pressure Calculation in Ball Valves Containing Bubbles

A method of analyzing bubbly flow in a ball valve in a hydraulic circuit is presented. The dynamics of a single bubble can be well described by a quasi-static approximation of the Rayleigh-Plesset equation. Hence the presence of bubbles in low volume fractions can be modeled through an effective compressibility of the flow, which is easy to implement in commercial CFD packages. In the sample valve, a volume fraction of 4% air bubbles results in a mass flux reduction of up to 10%, as the bubbles expand due to the pressure drop in the valve and partly block it. [DOI: 10.1115/1.1486220]

1 Introduction

A common type of valve in mobile hydraulic systems is the ball valve (see Bosch [1]). Basically, it consists of a cone-shaped seat, where a ball can be pressed into the seat by a spring or a magnetically actuated poppet, see Fig. 1. Applying a sufficiently large pressure difference across the valve, the force holding the ball in the seat will be overcome and the valve opens.

A frequent design requirement is to maximize the mass flux during the time the valve is open. Gas bubbles in the flow can counteract this aim, because they expand when entering the low pressure regime and thus partially block the valve.

The aim of the work presented in this paper was to investigate, by analysis and simulation, how gas bubbles and liquid interact and affect the functioning of the valve. A number of simplifications have been imposed. First, the bubbles are assumed to consist of air. Any vapor fraction in the bubbles is neglected. Second, the formation of new bubbles is not examined. Dissolution of air, due to local temperature or pressure changes, is neglected. Third, no investigations were made into the size of the bubble nuclei entering the valve. Bubbles with ambient radii between 20 and 200 μm are assumed to be present in the valve. For the sample valve in this article, the maximum bubble size is limited by the hydraulic circuit of which it is a part. A typical length scale of the valve is 1 mm. Further characteristics of this example problem are the high viscosity, $\mu = 0.27\ \mathrm{kg\,m^{-1}\,s^{-1}}$, the surface tension at the interface air-liquid, $\sigma = 0.035\ \mathrm{N\,m^{-1}}$, and a 4% volume fraction of air. The speed of sound in the liquid without bubbles is $c_l = 1493\ \mathrm{m\,s^{-1}}$ and the density is $\rho_l = 1092\ \mathrm{kg\,m^{-3}}$.

The paper first examines how a single bubble reacts to the pressure field in the valve. In Section 3, a density function is constructed which describes the density of the air-liquid mixture as a function of the pressure. This approach is possible only because Section 2 shows the bubble dynamics to be of secondary importance for the sample valve. If this were not the case, the density at a point in the flow field would depend on the pressure at that point *and* on the pressure history along the streamline through the point in question. As the streamline is the result of the flow field being calculated, some complicated iterative process would then be needed to solve the problem.

Determining the volume-averaged density is still not straightforward, because it should depend on the bubble size distribution. Due to the surface tension, the total volume occupied by the gas bubbles is nonlinearly dependent on the pressure. Some knowledge of the number of bubbles present and the initial values of their radius seems necessary. However, it will be shown that, for the size of bubble assumed to be present in the sample valve, different distributions of bubble size lead to almost the same result. So one may choose the simplest.

Being now supplied with a well-justified pressure-density relation for the bubbly flow in the valve, we perform, in Section 4, a full numerical simulation of the flow through the sample valve with a commercial CFD-Package. Conclusions will be contained in Section 5.

2 Calculations on a Single Bubble

We first focus on a single bubble. It is assumed that the bubble travels along a streamline through the valve. The local pressure on the bubble is used as input to determine the development of the bubble radius.

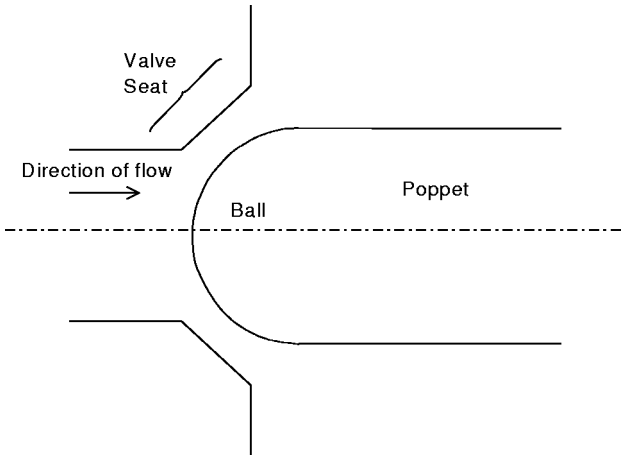

Fig. 1 Sketch of the main features of the ball valve

[1]Corresponding author.

Contributed by the Fluids Engineering Division for Publication in the JOURNAL OF FLUIDS ENGINEERING. Manuscript received by the Fluids Engineering Division May 19, 2000; revised manuscript received January 14, 2002. Associate Editor: Y. Matsumoto.

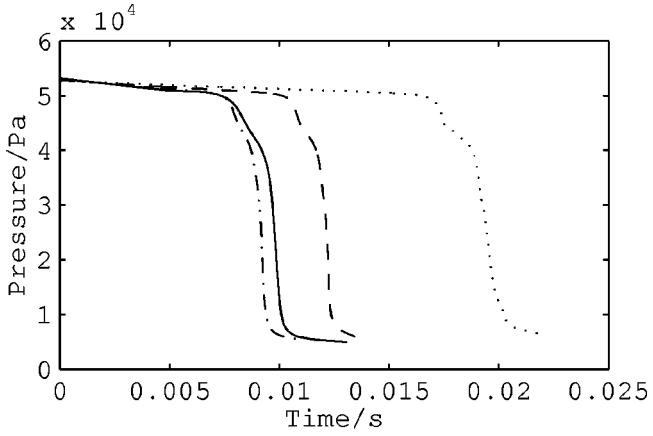

Fig. 2 Pressure development along four different streamlines in the example valve

2.1 The Driving Pressure of the Bubble. For the sample valve results of a 3D flow simulation were used to find the pressure along a streamline. The presence of the bubbles was not taken into account, but was based on a model for compressible flow.

Some examples of pressure development along streamlines through the valve in the fully open position are given in Fig. 2. The pressure drop occurs in two stages. The fluid motion through the valve has swirl and is not strictly rotational symmetric. Also a sealing lip in the seat of the sample valve makes the geometry and the flow more complicated. This leads to a pressure reduction in two stages, instead of the more straightforward pressure reduction one would get for a valve like the one in Fig. 1.

To be able to make some general statements, not limited to the present example, the bubble response is also calculated using some conceived functions as input, having the advantage that parameters can be varied.

As model function a pressure drop is taken, which is sufficiently smooth to pose no problems for the integration, see Fig. 3.

The pressures at the inlet and outlet of the ball valve are p_0 and p_1. This pressure drop occurs within a time interval Δt, being the time it takes the bubble to traverse the valve.

2.2 Bubble Dynamics. Using the terminology in Hilgenfeldt et al. [2], Leighton [3], and Brennen [4] the following equation will be referred to as the Rayleigh-Plesset equation:

$$\rho_l\left(R\ddot{R}+\frac{3}{2}\dot{R}^2\right)=p_{\text{gas}}-p_{\text{ext}}-\frac{4\mu\dot{R}}{R}-\frac{2\sigma}{R}+\frac{R}{c_l}\frac{d}{dt}p_{\text{gas}}. \quad (1)$$

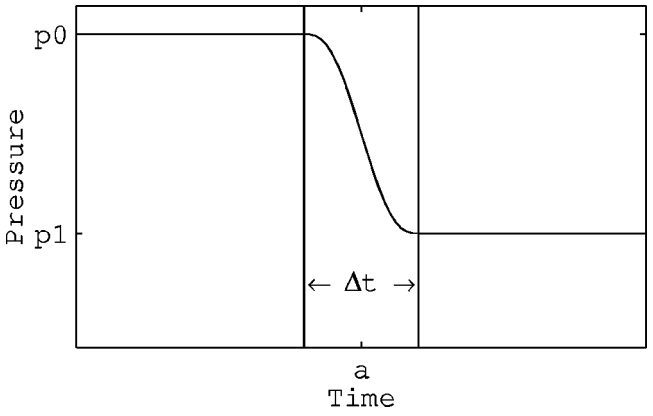

Fig. 3 Polynomial approximation of the pressure drop in the ball valve

Equation (1) takes the compressibility of the liquid into account to a limited extent, through the last term in the equation. This term represents the pressure associated with emitted sound waves.

As stated in the Introduction, two possible processes of mass transfer between fluid and bubble are neglected in the analysis: dissolution of air in/out the hydraulic liquid and evaporation/condensation of the hydraulic liquid.

The influence of phase changes of the hydraulic liquid is neglected, because the vapor pressure is much smaller than the pressure of air in the bubble. The values of the pressure before and after the valve are known (55,000 Pa and 5000 Pa respectively for the example). Since the value of the vapor pressure is of the order of several hundred Pa, it is reasonable to assume that the pressure never drops below the vapor pressure. The influence of gas dissolution is also neglected. The solubility is strongly dependent on temperature and weakly dependent on pressure. The temperature, however, remains constant in the example. Dissolved air can be released from the liquid by diffusion. The diffusion length scale is given by:

$$l=\sqrt{\pi D\Delta t}. \quad (2)$$

For the problem examined as an example, $D\sim 2.6\cdot 10^{-10}$ m^2 s^{-1}. Using a characteristic time scale of $\Delta t\sim 3\cdot 10^{-4}$ for the bubble dynamics, as calculated later on, the diffusion length scale is 0.5 μm, much smaller than the bubble radius: the influence of gas dissolution can therefore also be neglected.

The behavior of the pressure of the gas in the bubble is polytropic. Because the Péclet number $R\dot{R}/U\ll 1$, the isothermal limit (see Plesset and Prosperetti [5]) is considered:

$$p_{\text{gas}}=\frac{\left(p_0+\dfrac{2\sigma}{R_0}\right)(R_0^3-h^3)}{R^3-h^3}; \quad (3)$$

$h=R_0/8.85$ is the v.d. Waals' hard core radius.

The eigenfrequency ω of the bubble (Minnaert frequency) follows from linearizing the Rayleigh-Plesset equation (see Brennen [4]):

$$\omega^2=\frac{3R_1}{\rho_l}\left(p_0+\frac{2\sigma}{R_0}\right)\frac{(R_0^3-h^3)}{(R_1^3-h^3)^2}-\frac{2\sigma}{\rho_l R_1^3}. \quad (4)$$

A characteristic time scale based on the Minnaert frequency $\tau_c=2\pi/\omega$ will be needed later for comparison with other time scales, notably the time interval needed for the passage of the bubble through the valve.

The important aim of this research is to investigate how the bubble responds to a pressure drop: will the bubble expand and collapse violently (undesired) or does it exhibit a delayed expansion (favorable, since the expansion would take place behind the valve)? It will turn out that the latter is the case and that it is even possible to use a quasi-static approximation to describe the bubble behavior. This approximation, see e.g., Hilgenfeldt et al. [2], consists of dropping all derivatives with respect to time in the Rayleigh-Plesset equation

$$0=\left(p_0+\frac{2\sigma}{R_0}\right)\left(\frac{R_0^3-h^3}{R^3-h^3}\right)-\frac{2\sigma}{R}-p_{\text{ext}}(t), \quad (5a)$$

which is a simple fourth-order polynomial expression for $R(t)$.

Neglecting the hard core radius $h\ll R_0, R$, it reduces to a third-order polynomial

$$\frac{-p_{\text{ext}}(t)}{p_0}R^3-\frac{2\sigma}{p_0}R^2+\left(1+\frac{2\sigma}{R_0p_0}\right)R_0^3=0. \quad (5b)$$

In this approximation $R(t)$ can be given analytically in terms of $p_{\text{ext}}(t)$.

A concept used in the study of the acoustical behavior of bubbles is the Blake radius (see e.g., Hilgenfeldt et al. [2] or Leighton [3]). Bubbles smaller than the Blake radius display quasi-harmonically oscillating behavior, larger ones exhibit rapid

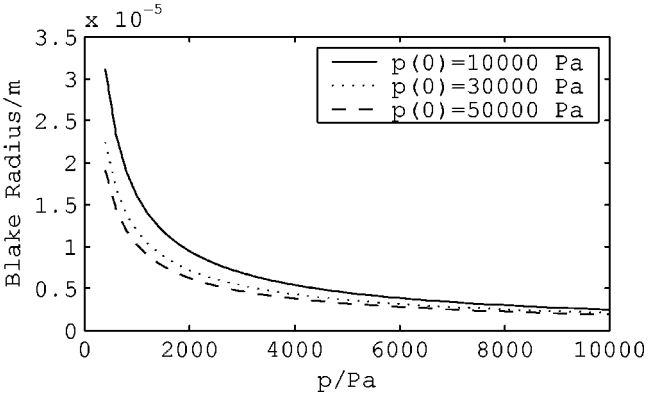

Fig. 4 Blake radius for different combinations of final and initial pressure

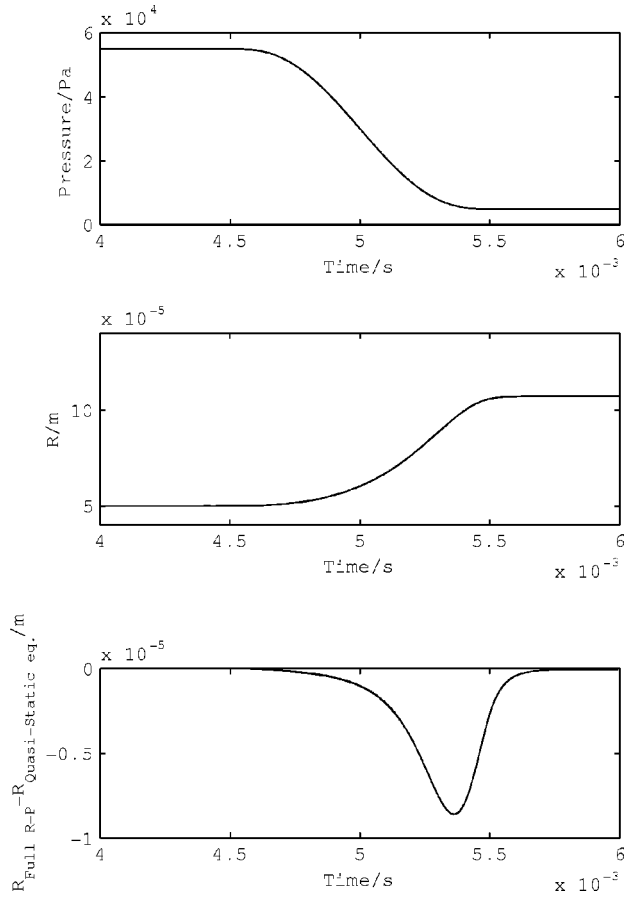

Fig. 5 Bubble radius response for a slow drop in pressure. $\Delta t = 1$ ms, $\tau_c = 28$ μs. (*a*) External pressure; (*b*) bubble radius development; (*c*) difference between the solution of the full Rayleigh-Plesset equation and the quasi-static approximation.

collapses. In the latter case, a complete description of the bubble behavior requires the use of the Rayleigh-Plesset Eq. (1), rather than Eq. (5).

The Blake radius as a function of the pressure amplitude can be calculated from Eq. (5*b*), see Eq. (3.4) in Hilgenfeldt et al. [6], and is displayed in Fig. 4. From that figure it can be concluded, that for the relatively small bubbles and small pressure amplitudes relevant to this study, the bubbles remain below the Blake threshold throughout.

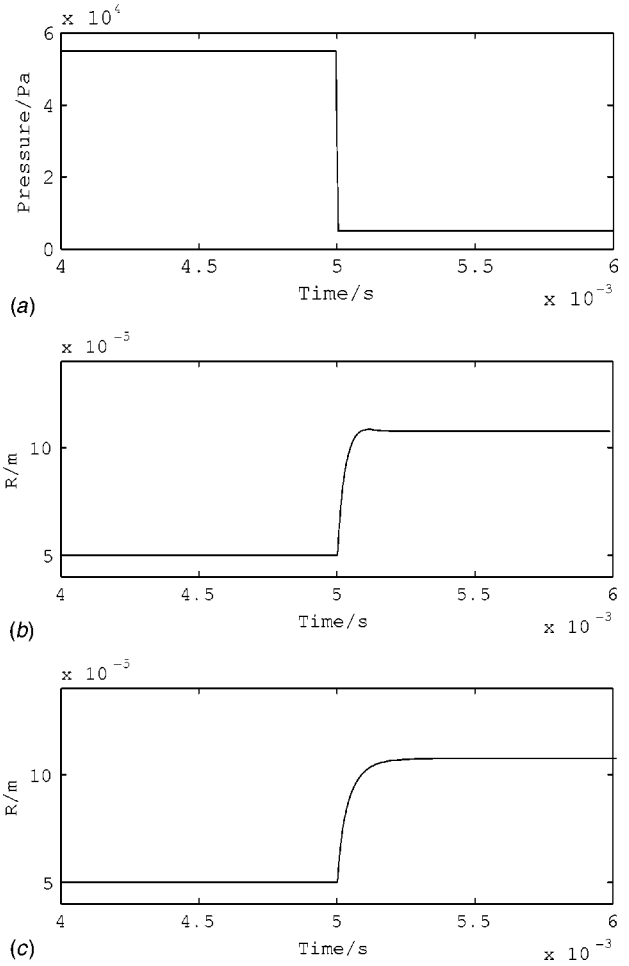

Fig. 6 Bubble radius response for a relatively steep drop in pressure. $\Delta t = 1$ μs, $\tau_c = 28$ μs. (*a*) External pressure; (*b*) bubble radius development for a relatively small value of the viscosity, $\mu = 0.17$ m^2 s^{-1}; (*c*) bubble radius development for a higher value of the viscosity, $\mu = 0.27$ m^2 s^{-1}.

To confirm this, the bubble dynamics were determined by numerically integrating the full ODE (1) with the model pressure function $p_{\text{ext}}(t)$ given in Fig. 3.

Three qualitative responses can occur, depending on the ratio of $\Delta t/\tau_c$ and on the value of the viscosity. Figures 5 and 6 show the response of a bubble with an initial radius of 50 μm. The bubble response is qualitatively independent of the initial bubble radius, but depends on the ratio of Δt and τ_c. If Δt is of the same order as τ_c or smaller, then the response will not follow the pressure closely. Figure 5 shows the bubble response for a pressure drop that occurs on a time scale comparable to that found along a streamline in the sample valve. The quasi-static approximation (5*b*) introduces only a small error, see Fig 5(*c*). The bubble response to steep pressure drops is shown in Fig. 6. If the viscosity is large, the bubble radius will lag behind the pressure, as in Fig. 6(*c*). For lower values of the viscosity, the bubble radius will exhibit overshoot, as demonstrated in Fig. 6(*b*). Figure 7 shows the bubble response to the pressure development actually found in the 3D simulation of the flow through the example valve. Larger pressure drops however can initiate much more violent bubble collapses and the quasi-static approximation would break down. Examples are jet cavitation (Cerutti et al. [7]), cloud cavitation (de Lange et al. [8]), edge cavitation (Young [9]), or sonoluminescence (Crum [10] and Brenner et al. [11]).

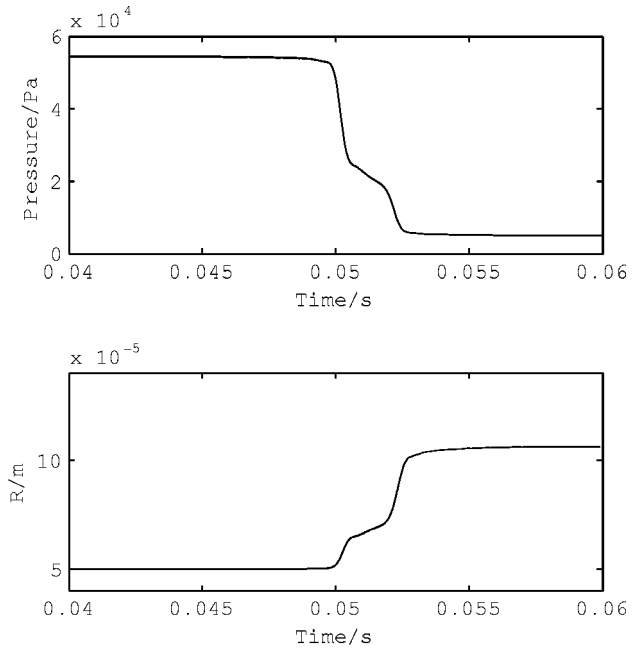

Fig. 7 Bubble radius response to the pressure development in the example valve. (*a*) External pressure; (*b*) bubble radius development.

2.3 Shape and Shape Stability. The Rayleigh-Plesset equation, describing the bubble in terms of its radius, assumes a spherical bubble. For the sample problem, some of the bubbles simply become too big to pass through the opened valve without deformation from the spherical shape. Another reason why the bubble might not be spherical is the pressure gradients in the seat area of the valve, leading to a pressure difference across the bubble, which might cause the bubble to lose its spherical shape. To estimate whether this is likely, a comparison with bubbles in a gravitational field is made by replacing in the usual Morton number $M=g\mu^4\Delta\rho/\rho^2\sigma^3$ and the Eötvös number $Eo=g\Delta\rho d^2/\sigma$ the buoyancy force per unit volume $g\Delta\rho$ simply by $|\nabla p|$. In addition to M and Eo, of course the Reynolds number $Re=\rho dU/\mu$ plays a role.

Clift et al. [12] give an overview which bubble shape to expect for a given set of values of the dimensionless variables. For the main flow area, away from the walls, pressure gradients in the sample valve are at most $4\cdot 10^7\ \mathrm{Pa\,m^{-1}}$. For the bubbles small enough to fit into the valve opening $Re<1$ and the Morton number is of order 4000, putting those bubbles firmly in the spherical range.

Finally, the stability of the bubble to shape perturbations is examined. This tests whether the bubble returns to a spherical shape after a distortion of this initial shape. Following the analysis of Hilgenfeldt et al. [2] or Prosperetti [13], we find that decay times for the perturbation were found between 0.001 and 0.005 s. In this analysis, homogeneous conditions inside the bubble have been assumed, thus neglecting heat losses, which cause extra damping, see Hao et al. [14] or Brenner et al. [15]. The spherical shape of the bubble is therefore very stable.

3 Modeling the Density of a Bubbly Fluid

In the quasi-static approximation, the volume of a bubble at a certain point only depends on the pressure *at that point*. One can therefore look for a function to describe the density of the mixture of air and liquid in relation to the pressure. If we take surface tension into account, then the density will depend on the distribution of initial bubble sizes. A general formula for the density of a mixture of bubbles and liquid, where the initial volume fraction of air is x, is the following:

$$\rho=\frac{\rho_0}{(1-x)+\int_{R_{0,\min}}^{R_{0,\max}} f(R_0)\frac{4}{3}\pi R^3(R_0,p;p_0,\sigma)dR_0}. \tag{9}$$

Here, the function $f(R_0)$, describing the distribution of ambient radii, is defined as:

$$x=\int_{R_{0,\min}}^{R_{0,\max}} f(R_0)\frac{4}{3}\pi R_0^3 dR_0. \tag{10}$$

The initial density of the mixture at pressure p_0 is denoted as ρ_0. The expression used for R, is the quasi-static approximation of Eq. (5). When also surface tension is neglected, the density becomes independent of the ambient bubble radius distribution, and the following expression is found for the density:

$$\rho=\frac{\rho_0}{1-x+x\cdot p_0/p}. \tag{11}$$

However, going one step further and including the surface tension term, the relation between p and ρ becomes dependent on the bubble size distribution. Two bubble size distributions will be considered; a uniform distribution of bubble radii and a Gaussian distribution.

3.1 Uniform Distribution of Bubble Radii. For a uniform bubble size distribution the properly normalized distribution function is

$$f(R_0)=\frac{4x}{R_{\max}^4-R_{0,\min}^4}\frac{3}{4\pi}$$

and the density is described by the:

$$\rho=\frac{\rho_0}{1-x+\frac{4x}{R_{0,\max}^4-R_{0,\min}^4}\int_{R_{0,\min}}^{R_{0,\max}} R^3(R_0,p;p_0,\sigma)dR_0} \tag{12}$$

The integral cannot be evaluated analytically. One could numerically evaluate Eq. (12), but within a CFD-program this would lead to higher calculation times. Therefore we employ an approximation which allows for an analytical solution. We rewrite Eq. (5) as

$$\frac{R_0^3}{R^3}-\frac{p}{p_0}=\frac{2\sigma}{p_0R_0}\left(\frac{R_0}{R}-\frac{R_0^3}{R^3}\right). \tag{13}$$

and linearize around the root of the right hand side. The expression resulting for R is plugged into (12), which is then integrated numerically.

Differences between this method, the full numerical evaluation of the density via (12), and the approximation (11), which neglects surface tension, only arise for low values of the pressure. The difference between the three functions describing the density is, however, at most 0.5% for the sample problem.

3.2 Gaussian Distribution of Bubble Radii. Next an expression describing the density, when the bubble radius distribution is a Gaussian, was also developed. A narrow Gaussian would correspond to a situation where all the bubbles have the same radius. It is opposite to the previous uniform distribution, where all the radii occur equally often.

For simplicity, it is assumed that all bubble radii from R_c down to 0 can initially occur. The density depends on the parameters R_c, the radius b corresponding to the maximum of the Gaussian and λ is a parameter used to set the width of the Gaussian. The expression for the density found in this way is:

$$\rho = \frac{\rho_0}{1 - x + x \cdot \int_0^{R_c} A \cdot \exp\left(\frac{(R_0 - b)^2 \ln \lambda}{(R_c - b)^2}\right) \cdot \frac{4\pi}{3} R^3(R_0, p; p_0, \sigma) dR_0}, \tag{14}$$

where A is defined as:

$$A = \frac{1}{\int_0^{R_c} \frac{4\pi}{3} R_0^3 \exp\left(\frac{(R_0 - b)^2 \ln \lambda}{(R_c - b)^2}\right) dR_0}. \tag{15}$$

The density as described by Eq. (14), was evaluated numerically in order to compare it to the one found from Eq. (11) (the function that neglects surface tension). For a broad Gaussian lying within the range of bubble sizes expected for the example problem, differences between the two functions amount to at most 1%. However, if all the bubbles are smaller than 20 μm, then the difference can be up to 10%. In the last case, one cannot get away with neglecting the surface tension. However, a broader distribution of larger bubbles is assumed in the valve and so for the numerical simulation we can use Eq. (11) as the pressure density relation, and this is what is implemented in the commercial CFD code.

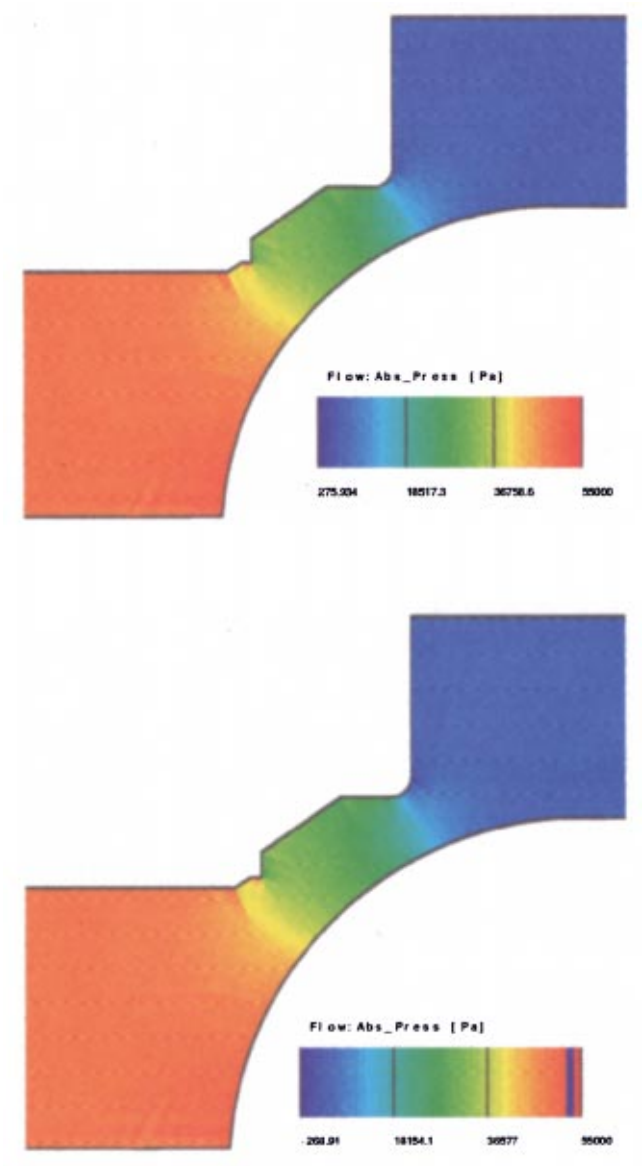

Fig. 8 Pressure field for the example valve. (*a*) With density function; (*b*) without density function.

4 Flow Simulations for the Example Ball Valve

The flow simulations alluded to in previous sections, were carried out using the commercially available CFD package AVL-Fire, a finite volume method. It is fully implicit, all terms containing no time derivatives are evaluated at the new time level. The spatial discretisation is of the hybrid type, switching between central and upstream differencing depending on the local cell Reynolds number. The velocity and pressure fields are linked by a SIMPLE (*S*emi-*I*mplicit *M*ethod for *P*ressure *L*inked *E*quations, see e.g., Ferziger et al. [16]). The resulting linear set of equations is solved by a Conjugate Gradient method for the velocity field. For the pressure a Gauss-Seidel method, combined with black-red SOR (*S*uccessive *O*ver *R*elaxation), is used.

The program can only carry out 3D flow simulations. It would have been possible to set up a geometry for the flow calculations based on the exact drawings of the valve. However, the geometry was simplified to a rotationally symmetrical valve. Only the flow in a 5 deg section was simulated. The program cannot switch to cylindrical coordinates, so the simplification could not really be exploited to the full extent. Indeed, taking such a small section creates a singularity at the valve axis, so the grid has to stop just short of the axis.

Although the flow field of interest is stationary, the flow simulation is that of a transient flow field. This has the advantage that the boundary conditions can be imposed gradually, to avoid sharp pressure gradients from occurring during the simulation. The final distribution of the pressure, resulting from the simulations for compressible two-phase flow, is given in Fig. 8(*a*). As pressure-density relation Eq. (11) was used, as justified in Sections 2 and 3. The pressure distribution in the incompressible monophase flow is given in Fig. 8(*b*).

In the compressible case, the mass flux is reduced by up to 10%, as shown in Fig. 9. This is a considerable amount for various applications. The reason is, of course, that incompressible flow can only respond to a pressure increase at the entrance of the valve by pushing the fluid through the valve, whereas compressible flow can also respond through compression, the bubbles being the origin of the effective compressibility here. This different behavior of compressible and incompressible flow can also be seen in the corresponding velocity fields in Fig. 10. The effect is most visible in the narrowest part of the valve, where a fluid particle experiences a pressure decrease and therefore expands in the compressible case, thus blocking the pathway and leading to a reduction of the velocity and the mass flow.

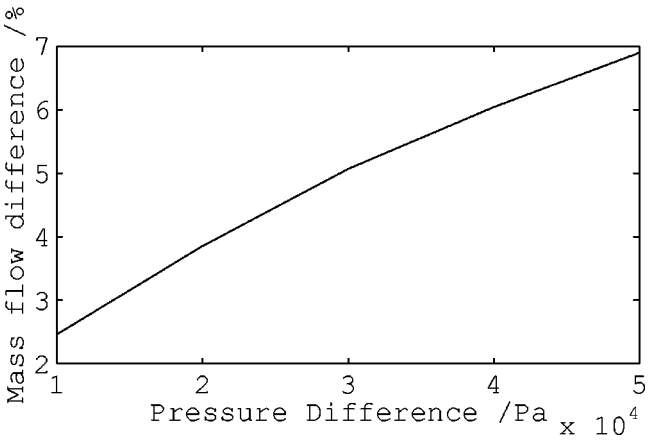

Fig. 9 Relative difference in the mass flow through the sample valve between the compressible and the incompressible calculation

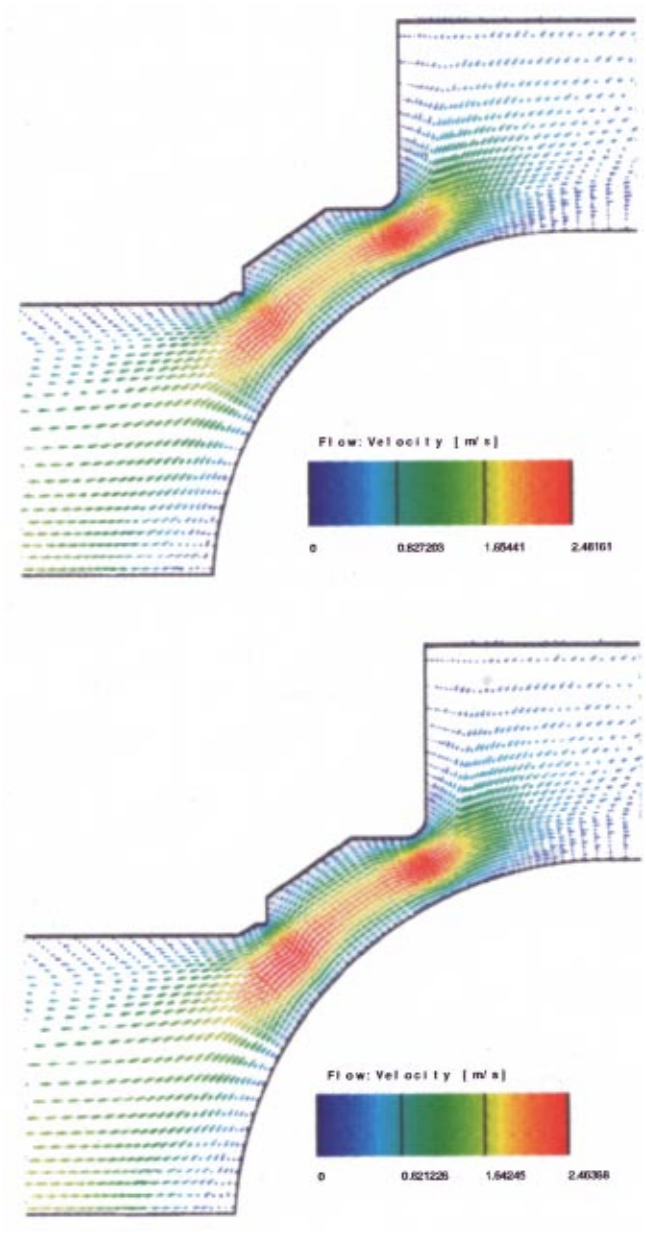

Fig. 10 Velocity vector field within the example valve. (*a*) With density function; (*b*) without density function.

5 Conclusions

In this work, the focus has been laid on calculations for a sample valve. In addition, some general conclusions concerning the procedure can be drawn, that are applicable to other ball valves as well.

First, one needs to have an idea of the properties of the bubbles. The content of the bubble was assumed to be air and a negligible amount of vapor. The size of these bubbles was determined by the dimensions of other elements in the hydraulic circuit. The amount of bubbles was determined from the measured volume fraction of air present.

The bubbles were assumed to be spherical, to be checked in retrospect. A means of doing this is to use perturbation analysis to investigate shape stability. Whether pressure gradients can lead to distortion, can be estimated by calculating the Reynolds number and the analogue of the Morton or Eötvös number. One should estimate, whether the geometry of the valve may lead to bubble deformations, as it obviously does, when the bubble gets too large to fit through the opened valve.

The next step is to specify the pressure drop over the valve, leading to the bubble expansion. The pressure experienced by the bubble as a function of time, is obtained by integrating the pressure along a streamline with a 3D code.

With that function describing the development of pressure in time, one can determine the development of the bubble radius in time. This was done for a number of model functions and for the pressure development extracted from the flow data. To determine the response of the bubble, the Rayleigh-Plesset equation was integrated.

For each bubble radius, a characteristic time scale can be calculated. The response of the bubble to the pressure drop depends on the ratio of the characteristic time scale and the time interval over which the pressure drops. For a fast pressure drop, the bubble can exhibit overshoot and will oscillate toward a final radius, if the viscosity is low. Alternatively, if the viscosity is high, the bubble can increase in size toward the final value, but lagging behind the pressure drop in time. If the pressure drop is not very steep, then the bubble response can be regarded as quasi-static. This is the case for the valve examined as an example. The time derivatives in the Rayleigh-Plesset equation can then be dropped, and one can employ the quasi-static approximation (5), where the presence of bubbles can be taken into account through a pressure-dependent density function.

The next step in the analysis is to find this expression for such a density function. We have shown that the distribution in initial bubble radius sizes has relatively little influence on the density function. If not all the bubbles are very small, surface tension can be neglected and one can use the simplest possible function to describe the density. It is a volume average over the liquid and the gas, neglecting the surface tension altogether. Such a description of the density of the hydraulic liquid with bubbles in it, is easy to implement in commercially available CFD codes like the AVL-Fire code used here.

For the sample valve the presence of bubbles in the flow, causing the effective compressibility, has a considerable blocking effect, reducing the mass flux by up to 10%. The reason is that the bubbles expand when experiencing the decrease of pressure in the valve and thus partly block the flow through the narrowest part of the valve.

In summary, one can see that the combination of parameters in the example valve is very favorable. It has turned out that one can take account of the presence of bubbles in a very simple way. In retrospect, splitting the problem into two parts, namely looking at the influence of bubbles on the flow and that of the flow on the bubbles separately, could have been avoided. Such a split has, however, been necessary just to prove this very fact.

References

[1] Bosch GmbH. R., 1995, ''*Kraftfahrttechnisches Handbuch*,'' 22nd edition.
[2] Hilgenfeldt, S., Lohse, D., and Brenner, M. P., 1996, ''Phase Diagrams for Sonoluminescing Bubbles,'' Phys. Fluids, **8**(11), pp. 2808–2826.
[3] Leighton, T., 1994, *The Acoustic Bubble*, Academic Press, London.
[4] Brennen, C. E., 1995, *Cavitation and Bubble Dynamics*, Oxford University Press, New York.
[5] Plesset, M., and Prosperetti, A., 1977, ''Bubble Dynamics and Cavitation,'' Annu. Rev. Fluid Mech., **9**, pp. 145–185.
[6] Hilgenfeldt, S., Brenner, M. P., Grossmann, S., and Lohse, D., 1998 ''Analysis of Rayleigh-Plesset Dynamics for Sonoluminescing Bubbles,'' J. Fluid Mech. **365**(10), pp. 171–204.
[7] Cerutti, S., Knio, O. M., and Katz, J., 2000, ''Numerical Study of Cavitation Inception in the Near Field of an Axisymmetric Jet at High Reynolds Number,'' Phys. Fluids, **12**(10), pp. 2444–2460.
[8] de Lange, D. F., de Bruin, G. J., and van Wijngaarden, L., 1993, ''Observations of cloud cavitation on a stationary 2D profile,'' Proc. IUTAM Symp.: Bubble Dynamics and Interface Phenomena, J. Blake et al., eds., Kluwer, pp. 241–246.
[9] Young, F. R., 1999, *Cavitation*, Imperial College Press, London.
[10] Crum, L., 1994, ''Sonoluminescence,'' Phys. Today, **47**(9), pp. 22–29.

[11] Brenner, M., Hilgenfeldt, S., and Lohse, D., 2002, ''Single-Bubble Sonoluminescence,'' Rev. Mod. Phys., **74**(2), pp. 425–484.
[12] Clift, R., Grace, J., and Weber, M., 1978, *Bubbles, Drops and Particles*, Academic Press, London.
[13] Prosperetti, A., 1977, ''Viscous Effects on Perturbed Spherical Flows,'' Q. Appl. Math., **25**, pp. 339–352.
[14] Hao, Y., and Prosperetti, A., 1999, ''The Effect of Viscosity on the Spherical Stability of Oscillating Gas Bubbles,'' Phys. Fluids, **11**(6), pp. 1309–1317.
[15] Brenner, M., Dupont, T., Hilgenfeldt, S., and Lohse, D., 1998, ''Reply on a Comment,'' Phys. Rev. Lett., **80**, pp. 3668–3669.
[16] Ferziger, J. H., and Peric, M., 1996, *Computational Methods for Fluid Dynamics*, Springer, Berlin.